

# Hard X-Ray Reflectivity Of Spherically Bent Mica Crystals

M. Sánchez del Río<sup>1</sup>, A. Ya. Faenov<sup>2</sup>, T.A. Pikuz<sup>2</sup>, A. Souvorov<sup>1</sup> and A.K. Freund<sup>1</sup>

<sup>1</sup>European Synchrotron Radiation Facility, BP 220, 38043 Grenoble Cedex, France

<sup>2</sup>Multicharged Ions Spectra Data Center of VNIIFTRI, Mendeleevo, Moscow region  
141570 Russia

**Abstract.** Mica crystals are used as soft x-ray and neutron monochromators, as well as for imaging applications, in particular for plasma x-ray diagnostics. Although the d-spacing for mica is large ( $2d=19.88 \text{ \AA}$ ), it can be used for hard x-ray applications by exploiting the large number of intense high diffraction orders. We have measured diffraction profiles of mica crystals at the ESRF BM5 beamline to study the suitability of these crystals for hard x-ray applications. Two good quality mica crystal curved following a spherical shape with curvature radii of 10 and 15 cm were analyzed. A micrometry incident beam was prepared to avoid smearing the rocking curve with the angular spread induced by the beam projection on the crystal surface. Many diffraction orders from with indices from (0,0,6) to (0,0,38) were recorded at photon energies of 12, 16 and 20 keV.

## INTRODUCTION

Many different varieties of micas can be found in Nature [1]. Several determinations of their atomic arrangements have been done. [2]. Most of them present similar d-spacing ( $2d = 19.88 \text{ \AA}$ ) and relatively low reflection coefficient due to the presence of low-Z elements. Because of that, mica does not appear as an optimistic candidate for hard x-ray applications. However, mica has the rare property of reflecting x-rays almost equally in several (including quite high) diffraction orders. Therefore, using high harmonics, the spectral range of applicability of mica is largely extended. High quality bent mica crystals, with spherical, toroidal or cylindrical curvature, are widely used for imaging applications in association with plasma x-ray sources: they can be used as plasma analyzers [3,4], backlighting schemes [5] and also to exploit the plasma sources as x-ray sources for different applications, e.g., mica curved crystals can be used to produce quasi parallel (with divergence up to 1 mrad) beams by using a plasma source [6], and for microscopical applications [7]. Mica crystals are also widely used as neutron instruments [8]. For synchrotron radiation applications, they can be used as soft x-ray monochromators or as crystal analyzers (e.g., for micro x-ray fluorescence applications [9]).

In this work we present hard x-ray reflection profiles for two spherically curved mica samples that have already been used for plasma applications. The objective is to record experimental information that could help in assessing the usability of these

crystals for a given application. In order to record the diffraction profiles of the curved crystals (with curvature radii of 10 and 15 cm), a monochromatic collimated beam with a small cross section is required to use. These conditions were fulfilled at the ESRF BM5 beamline.

## EXPERIMENTAL RESULTS

The experiments were performed at ESRF beamline BM5. The source was an ESRF bending magnet with critical energy of 19 keV. The beamline is equipped with a double plane crystal Si (1,1,1) monochromator delivering a monochromatic beam with resolving power of about  $10^4$ . An entrance slit upstream from the sample defined a beam with cross section of 8  $\mu\text{m}$  (horizontal) and 470  $\mu\text{m}$  (vertical). The mica sample was mounted in a diffractometer. The diffraction plane was horizontal. The rocking curves were measured by performing standard  $\theta$ - $2\theta$  scans. A scintillator detector was used to record the diffracted intensity. The experiments were done using monochromatic radiation of 12, 16 and 20 keV. Two mica samples were studied, with curvature radii of 10 and 15 cm, respectively. The rocking curves, as shown in Fig. 1, have the typical triangular or trapezoidal shape. In both cases, the atomic layers which are closer to the surface reflect strongly. They are responsible for the peak reflectivity values. The atomic layers that are found deeper in the crystal bulk are slightly disoriented (non-parallel) with respect to those close to the surface, due to the curvature. Therefore, the beam arrives onto them with a slightly different incident angle. In addition, the attenuation is more important for deeper layers, thus giving lower reflectivity. This explains the triangular profile. When the crystal is thinner than the distance that beam would penetrate into the crystal, a part of the “triangle” is missing, and the profile shows a trapezoidal shape.

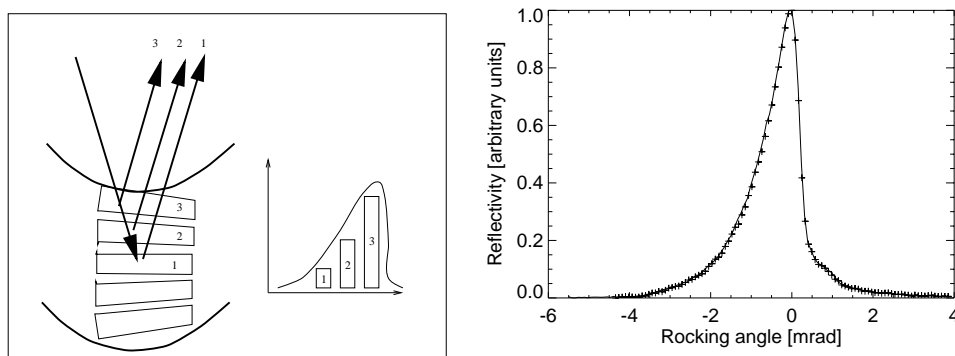


**FIGURE 1.** Left: schematic interpretation of how different blocks of atomic layers will contribute to the form a triangular diffraction profile (see text). Right: rocking curve for the (4,0,0) reflection of a mica sample with  $R=10$  cm at 12 keV. The continuous line is the angular scan. The + symbol refers to a linear scan of the crystal divided by the curvature radius (see text).

The experimental rocking curve is a convolution of the diffraction profile with the beam divergence. With an ideal pencil beam (no divergence, zero cross section, and infinite resolving power), both the rocking curve and the diffraction profile match perfectly. The width of the diffraction profile for a bent crystal is several times the Darwin width. In our case this is of the order of few tens of mdeg, depending on the curvature, photon energy, and Miller indices. It is then crucial to reduce the overall beam divergence to quantities on this order or smaller. The effective beam divergence comes from two factors: i) the divergence of the photon beam  $\Delta_1$ , which is negligible in our case ( $\Delta_1 = (\text{slit size}) / (\text{source distance}) = 8 \cdot 10^{-6} / 40$ ), and ii) the angular spread produced by the projection of the beam cross section onto the curved crystal surface. The latter produces a dispersion of the Bragg angle with a value of  $\Delta_2 = (s/\sin\theta_B)/R$ , being  $s$  the size of the entrance slit in the direction of the diffracting plane,  $\theta_B$  the Bragg angle and  $R$  the bending radius. In our case  $s=8\mu\text{m}$ ,  $\theta_B>5$  deg,  $R>10$  cm, thus the added divergence is, in the worst case, about  $10^{-3}$ , i.e., 50 mdeg.

Our samples show a very uniform curvature, demonstrated by their performances in other applications. We have tested the crystal curvature by comparing two diffraction profiles: i) the first one recorded in the usual way ( $\theta$ - $2\theta$  scan), and ii) keeping fixed the incident beam and moving the crystal along a direction perpendicular to the crystal surface, and which lies in the diffraction plane. Therefore, the grazing angle changes continuously due to the crystal curvature. Both profiles (see Fig 1) showed an identical shape. The longitudinal scan can be related to the angular scan if we know the radius of curvature. From the comparison of both spectra we obtained a  $R=12.2$  cm, close to the nominal value of 10 cm.

In order to compare the different curves, we have kept the gain of the detector to the same value with dynamical range optimized for the more intense rocking curves. However, we could not measure the direct beam because the detector was saturated. We measured it using some attenuators, but the experimental attenuation does not fit with the theoretical value, due probably to inelastic effects, impurities, variation in thickness, etc. Therefore, we present here the experimental data normalized to the data of a given harmonic. More precise measurements should be done to normalize the reflectivity to the incident intensity.

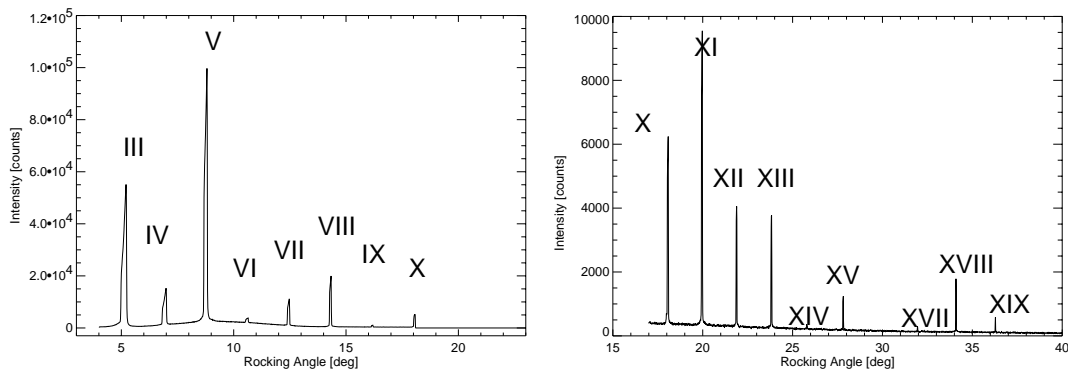


**FIGURE 2.** Wide scans for mica sample with  $R=15$  cm at 20 keV showing the different diffraction orders and their relative intensities.

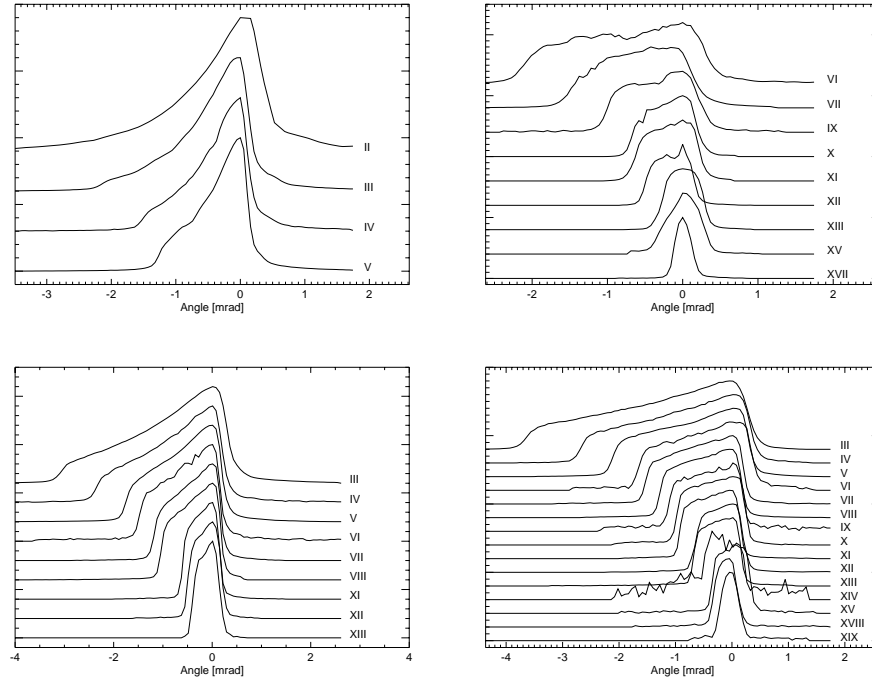


**FIGURE 3.** Rocking curves for the two mica samples: i) R=10cm at 12 keV ( top left panel) and 16 keV (top right panel) and, ii) R=15cm at 16 keV (bottom left) and 20 keV (bottom right). For improving the visualization, the zero angle is set to the maximum of the profile, and each curve is normalized to its particular peak value. Relative peak values are shown in Table 1.

**TABLE 1. Peak (P), Full Width at Half Maximum in mrad (W) and Integrated reflectivities (I), for the different mica harmonics (or reflections). Peak and integrated intensity values are normalized to the V harmonic for the sample with R=10 cm at 12 keV, and to the VII for all other cases.**

| crystal sample with R=15 cm |      |                    |                    |      |                    | Har-<br>monic    | crystal sample with R=10 cm |                  |                    |        |                    |  |
|-----------------------------|------|--------------------|--------------------|------|--------------------|------------------|-----------------------------|------------------|--------------------|--------|--------------------|--|
| 16 keV                      |      |                    | 20 keV             |      |                    |                  | 12 keV                      |                  |                    | 16 keV |                    |  |
| P/P <sub>VII</sub>          | W    | I/I <sub>VII</sub> | P/P <sub>VII</sub> | W    | I/I <sub>VII</sub> | P/P <sub>V</sub> | W                           | I/I <sub>V</sub> | P/P <sub>VII</sub> | W      | I/I <sub>VII</sub> |  |
| 9.12                        | 1.81 | 17.02              | 4.95               | 2.67 | 8.67               | III              | 0.92                        | 0.86             | 1.22               |        |                    |  |
| 1.38                        | 1.57 | 2.12               | 1.32               | 2.50 | 1.95               | IV               | 0.15                        | 0.73             | 0.16               |        |                    |  |
| 9.58                        | 1.54 | 12.61              | 9.07               | 2.29 | 11.67              | V                | 1.00                        | 0.70             | 1.00               |        |                    |  |
| 0.17                        | 1.50 | 0.21               | 0.19               | 1.95 | 0.22               | VI               |                             |                  | 0.21               | 2.27   | 0.28               |  |
| 1.00                        | 1.24 | 1.00               | 1.00               | 1.68 | 1.00               | VII              |                             |                  | 1.00               | 1.54   | 1.00               |  |
| 1.90                        | 1.15 | 1.76               | 1.85               | 1.41 | 1.61               | VIII             |                             |                  |                    |        |                    |  |
|                             |      |                    | 0.08               | 1.29 | 0.07               | IX               |                             |                  | 0.06               | 1.20   | 0.04               |  |
|                             |      |                    | 0.49               | 1.22 | 0.39               | X                |                             |                  | 0.43               | 0.82   | 0.22               |  |
| 0.71                        | 0.73 | 0.45               | 0.76               | 1.06 | 0.51               | XI               |                             |                  | 0.60               | 0.82   | 0.32               |  |
| 0.30                        | 0.66 | 0.17               | 0.34               | 0.84 | 0.19               | XII              |                             |                  | 0.32               | 0.61   | 0.12               |  |
| 0.29                        | 0.52 | 0.13               | 0.32               | 0.82 | 0.18               | XIII             |                             |                  | 0.28               | 0.54   | 0.11               |  |
|                             |      |                    | 0.01               | 0.72 | 0.01               | XIV              |                             |                  |                    |        |                    |  |
|                             |      |                    | 0.10               | 0.66 | 0.05               | XV               |                             |                  | 0.07               | 0.52   | 0.02               |  |
|                             |      |                    |                    |      |                    | XVII             |                             |                  | 0.15               | 0.24   | 0.03               |  |
|                             |      |                    | 0.15               | 0.42 | 0.05               | XVIII            |                             |                  |                    |        |                    |  |
|                             |      |                    | 0.04               | 0.35 | 0.01               | XIX              |                             |                  |                    |        |                    |  |

Fig. 2 shows wide scans where it is possible to compare the relative intensity for the different harmonics. The harmonics I and II (reflection (0,0,2) and (0,0,4),

respectively) were not accessible in our configuration. The higher measured intensities correspond to harmonics V and III. The main results are shown in Table 1, where the relative peak intensities, integrated intensities, and rocking curve width for all the measures profiles. All normalized rocking curves are shown in Fig. 3. Although we do not give absolute reflectivity, because of the mentioned problem, we can roughly estimate that for the sample with R=10 cm, the peak normalization value at the V harmonic at 12 keV would correspond to about 55% of the incoming intensity. For both samples at 16 keV, the peak for the VII harmonic is about 1% of the incoming intensity.

In conclusion, it would be possible to use mica crystals as x-ray monochromators, for imaging applications, or for focusing applications, with an acceptable efficiency (few per cent transmission) by selecting an adequate diffraction order. They could be more suitable for softer x-rays, especially around 1 keV, where other crystals have difficulties to work.

Correspondence and requests for materials should be addressed to A. Ya. Faenov (e-mail: faenov@yahoo.com)

## REFERENCES

1. See, for example, <http://web.wt.net/~daba/Mineral/dana/VIII-71.html#71.2>
2. R.W.G. Wyckoff, "Crystal Structures" Interscience Publ. 1965
3. A. Ya. Faenov, S. A. Pikuz, A. I. Erko, B. A. Bryunetkin, V.M. Dyakin, G.V. Ivanenkov, A. R. Mingaleev, T. A. Pikuz, V.M. Romanova and T.A. Shelkovenko, *Physica Scripta* **50**, 333-338 (1994)
4. S.A. Pikuz, A.Ya. Faenov, T.A. Shelkovenko, D.A. Hammer, A.Ya. Faenov. *Physica Scripta*, **51**, 517 (1995)
5. M. Sanchez del Rio, A.Ya. Faenov, V.M. Dyakin, T.A. Pikuz, S.A. Pikuz, V.M. Romanova, T.A. Shelkovenko. *Physica Scripta*, **55**, 735 (1997).
6. M. Sanchez del Rio, M. Fraenkel, A. Zigler, A. Ya. Faenov and T. A. Pikuz, *Rev. Sci. Instrum.* **70**, 1614-1620 (1999)
7. T.A. Pikuz, A. Ya. Faenov, M. Fraenkel, A. Zigler, F. Flora, S. Bollanti, P. Di Lazzaro, T. Letardi, A. Grilli, L. Palladino, G. Tomassetti, A. Reale, L. Reale, A. Scafati, T. Limongi and F. Bonfigli, *SPIE proceedings* **3767**, (1999)
8. M. L. Crow, *Physica B* **241-243**, 110-112 (1998)
9. Z. W. Chen, *SPIE proceedings* **3767**, (1999)